ISSN 0022-4766, Journal of Structural Chemistry, 2019, Vol. 60, No. 4, pp. 583-601. © Pleiades Publishing, Inc., 2019.
Russian Text © The Author(s), 2019, published in Zhurnal Strukturnoi Khimii, 2019, Vol. 60, No. 4, pp. 609-628.

ELECTRONIC AND CRYSTAL STRUCTURES OF NITROGEN-CONTAINING ELECTROCONDUCTIVE AND ELECTROACTIVE POLYMERS

Ya. O. Mezhuev, Yu. V. Korshak, M. I. Shtilman, and S. E. Pokhil

Current ideas about the electronic and crystal structures of nitrogen-containing conductive polymers are considered. A comparative critical analysis of literature data on electronic, vibrational, and NMR spectra for different nuclei, and X-ray diffraction data for various forms of polyaniline, polyphenylenediamine, and polypyrrole is presented. Particular attention is paid to the relationship between the electronic and crystal structure of nitrogen-containing polyconjugated systems and their electrical conductivity.

DOI: 10.1134/S0022476619040097

Keywords: polyaniline, polypyrrole, electroconductive polymers, polyphenylenediamine, spectroscopy.

INTRODUCTION

Polyconjugated systems have a number of unique physicochemical properties to be used in electronics, biomedical applications, production of sensor systems, and as coatings providing a number of specific surface properties [1]. Nitrogen-containing conductive and electroactive polymers (including polymers of aromatic amines and pyrroles) are one of the most important classes of polyconjugated systems in terms of their practical applications [1] due to the simplicity of preparation methods, high chemical and thermal stability [2-4]. Nitrogen-containing conductive polymers are obtained by oxidative polymerization and copolymerization of aniline derivatives [5-19], phenylenediamines [6, 20-27], and pyrrole [28-33]. Oxidative polymerization of aromatic amines and pyrroles can be initiated by the action of various chemical oxidizing agents (persulfates, permanganates, dichromates, chromates, salts of some transition metals in higher oxidation states) [32-41], enzymes [42-44], and by electrochemical methods [1, 29, 30, 45-50]. The resulting polymers are active in redox processes [51-53] and, in the case of polyaniline, also in acid-base equilibria [54, 55]. A wide range of possible applications of this class of polymers and a sustained interest to their study are due to the participation of nitrogen-containing conductive and electroactive polymers in acid-base and redox equilibria, marked dependence of their properties on the position of these equilibria, and substantial electrical conductivity that some of them exhibit in the doped state. Since the mid-1980s, the variety of possible forms of nitrogen-containing conductive polymers stimulated rapid development of research aimed at establishing relationships between the features of their electronic and crystal structures and the positions of their acid-base and redox equilibria.

Mendeleev University of Chemical Technology of Russia, Moscow, Russia; valsorja@mail.ru. Original article submitted April 05, 2018; revised November 12, 2018; accepted November 12, 2018.

When considering the structure of polypyrrole chains, which are active in redox transformations, usually three types of chain fragments are distinguished according to their oxidation degree: non-oxidized chain sites (neutral fragments), polarons (radical cations), and bipolarons (dications). The proportion between the chain fragments depends on the conditions of pyrrole oxidative polymerization and the nature of electrochemical polypyrrole post-processing (Scheme 1) [53].

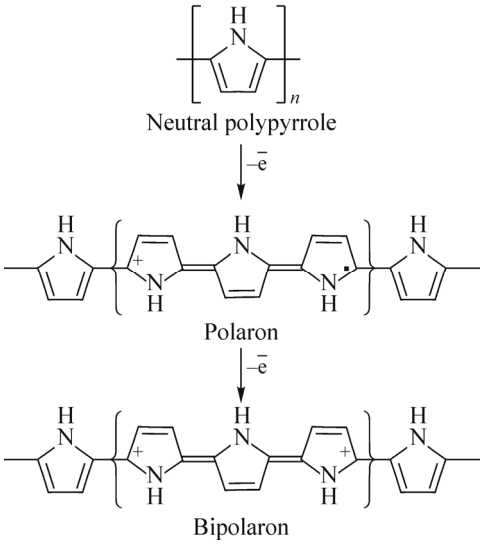

Scheme 1.

For polyaniline, three main states are also commonly considered: leucoemeraldine, emeraldine and pernigraniline differing in the ratio of their aminobenzoic and quinone diimine fragments (Scheme 2A) so that each of them has corresponding base and salt forms (Scheme 2B) [56]. Quinone diimine fragments are formed by the oxidation of aminobenzoic fragments (Scheme 2B).

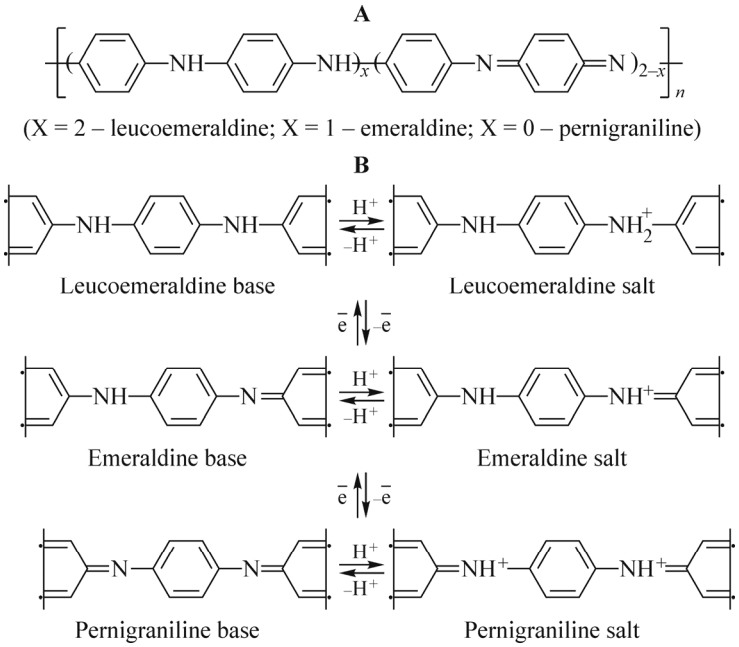

Scheme 2.

Protonation of the leucoemeraldine base proceeds along the secondary amino group. In the presence of quinone imine fragments in the chain, protonation proceeds along the more basic imine nitrogen atom. Two bipolarons are introduced into the chain during the protonation of quinone imine fragments and, being unstable, further transform into polarons (Scheme 3) [57, 58].

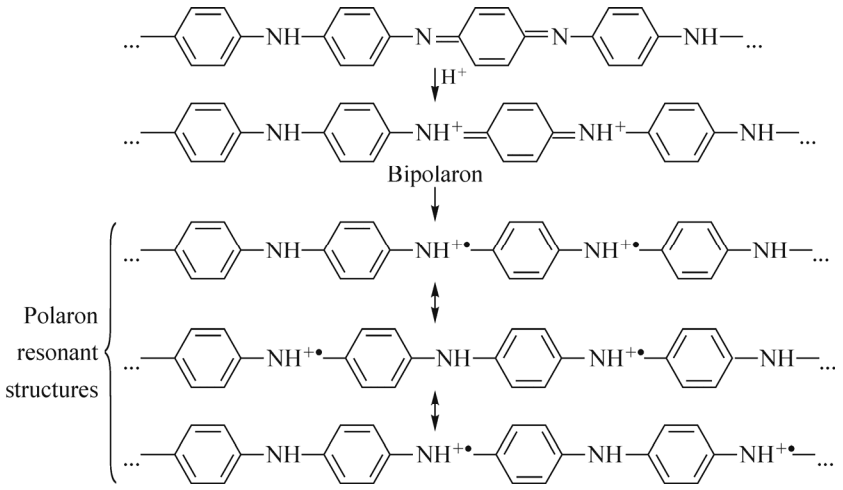

Scheme 3.

The variety of possible chain fragments in aromatic diamine polymers is even greater due to the possibility of cycle formation during polymerization [20-27, 59, 60]. Thus, it is believed that polymerization of all phenylenediamines is associated with the formation of similar structure products whose chains contain oligophenazine cyclic fragments, sometimes separated by acyclic fragments (Scheme 4). Poly(*n*-phenylenediamine) chains are mainly built of fragments I and II, while poly(*o*-phenylenediamine) chains contain also significant amounts of fragments III. The predominance of acyclic fragments over oligophenazine fragments in the course of oxidative polymerization of *o*-phenylenediamine and *n*-phenylenediamine has been reported only in a few cases. During polymerization of *m*-phenylenediamine, chain branching and stitching are often observed along with the formation of phenazine fragments. Polymers of aromatic diamines, as well as those of aromatic monoamines, are active not only in redox processes but also in protolytic equilibria, which greatly expands the range of their possible chain fragments.

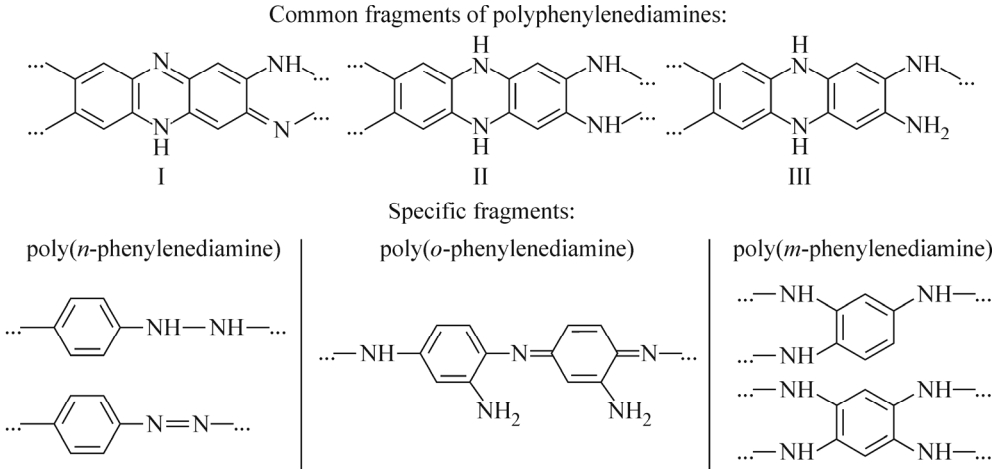

Scheme 4.

Even though almost all original works on the synthesis and use of nitrogen-containing electrically conductive polymers mention the aspects concerning their electronic and crystal structures, there have yet been no review papers summarizing the results of this important field of research. The present work not only concerns the problem of electronic and crystal structure of nitrogen-containing electrically conductive and electrically active polymers but also aims at summarizing and critical analysing the results accumulated in this area over the past thirty years.

ELECTRONIC STRUCTURE OF NITROGEN-CONTAINING ELECTROCONDUCTIVE AND ELECTROACTIVE POLYMERS

Since the electronic structure of nitrogen-containing electrically conductive and electroactive polymers is usually studied by a complex of spectral methods such as UV, IR, and NMR spectroscopy, this section is devoted to the discussion, analysis, and generalization of results obtained with these methods.

For polyaniline, the nature of absorption in UV and visible regions of the spectra is determined mainly by the level of chain oxidation and the position of the protolytic equilibrium. The electronic spectrum of emeraldine base exhibits two absorption maxima at 325 nm and 625 nm [61]. The shortwave band at 325 nm corresponds to the π–π^* transition, while the longwave band at 625 nm corresponds to the complex formation associated with a charge transfer between quinone diimine (acceptor) and aminobenzoic (donor) fragments of different chains resulting in the formation of low-lying vacant π orbitals [1].

The formation of the complex associated with a charge transfer between quinine diimine and aminobenzoic fragments of different chains of emeraldine base apparently explains its low solubility in the great majority of solvents. Also, the energy of interchain interactions should be greatly contributed by the formation of a system of hydrogen bonds. As a result, the emeraldine base is soluble only in certain bipolar aprotic solvents (N,N′-dimethylformamide, dimethyl sulfoxide, and N-methyl pyrrolidone) [62, 63] which simultaneously possess high dielectric permittivity and behave as chaotropic agents so that the solubility of the emeraldine base is smaller than that of leucoemeraldine.

Protonation of the emeraldine base with inorganic acids leads to the formation of emeraldine salts which are not soluble in any solvent [1]. Apparently, this is the result of the well-known inability of ammonium salts to form hydrogen bonds. Thus, the protonation of the emeraldine base results primarily in weakening the interactions between the fragments of the polymer chain and the solvent, while maintaining fairly strong interchain interactions. The inability of a part of N–H groups of the emeraldine salt chain to form hydrogen bonds results in the weakening of both interchain interactions and "polymer–solvent" interactions; however, the solubility is decreased due to the preservation of significant interchain interactions. In terms of interchain interactions, which are realized only through hydrogen bonding, it is difficult to explain the fact that the emeraldine base in N-methylpyrrolidone has lower solubility than the leucoemeraldine base which contains a greater number of secondary amino groups capable to form hydrogen bonds both between the chains and between the fragments of the polymer chain and the solvent.

Thus, although a great majority of works explain the solubility variation in different polyaniline forms in terms of hydrogen bond formation, this interpretation is not complete and requires also taking into account the interchain interactions which result from complex formation involving charge transfer. At the same time, formation of interchain hydrogen bonds allows explaining the increase of the solubility of the emeraldine base in the presence of typical chaotropic agents such as lithium chloride [64] or 2-methylaziridine [65] as well as the fact that pernigraniline base and salt forms (first of them does not contain N–H bonds and the second contains only N–H salt bonds) are not soluble in any solvent.

Finally, the existence of a complex involving charge transfer between aminobenzoic and quinone diimine fragments of different chains indicates the existence of a complex with a charge transfer between quinone diimine fragments and the monomer (Scheme 5). It should be formed as a result of oxidative polymerization of aniline underlying the polyaniline synthesis. The hypothesis about the existence of a complex involving charge transfer between the monomer and quinone imine fragments of the formed polymer chains was first put forward by the authors of this review and discussed in detail in

[66-69] to explain the nature of the autoacceleration of the oxidative polymerization of aromatic amines and to describe quantitatively the kinetics of the process.

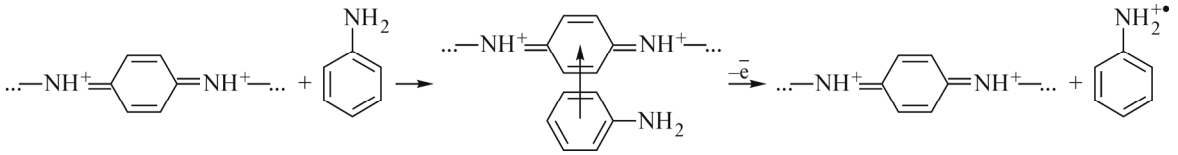

Scheme 5.

When doped with hydrochloric acid, the emeraldine base exhibits absorption band shifts and the occurrence of a new band in the long-wavelength region. For example, the electronic spectrum of emeraldine hydrochloride contains absorption peaks at 340 nm, 440 nm, and 800 nm [61]. At the wavelengths greater than 800 nm, emeraldine salts show an intense shoulder of the longwave absorption band. The absorption band at 340 nm corresponds to the π–π* transition, while those at 440 nm and 800 nm are assigned to the mobility of π polarons and π* polarons [70].

According to the study of the electronic spectra of emeraldine thin films [71], the ratio of absorbances at 950 nm and 630 nm increases together with the protonation degree, which confirms the above assignment of absorption bands in the electronic spectra of emeraldine salt and base forms.

The electronic spectrum of the pernigraniline base contains two absorption bands at 320 nm (π–π* transition) and 530 nm (the Peierls transition), and the long-wavelength band shifts to 700 nm as a result of protonation.

The assignment of the shortwave band to π–π* transitions is confirmed by the absence of long-wavelength absorption bands in the electronic spectrum of leucoemeraldine, which has no quinone imine fragments in its chain. The electronic spectra of leucoemeraldine base and salt forms contain single absorption peaks at 325 nm and 300 nm, respectively [72]. According to the authors of the work, a slight hypsochromic shift of the absorption band observed during the protonation of the leucoemeraldine base can be explained by reduced length of conjugated chain segments, since the quaternized nitrogen atom of the secondary amino group shows no mesomeric effect.

It is also noteworthy that the oxidation of leucoemeraldine by air results in the occurrence of an absorption band with a peak at 425 nm, which is characteristic of the emeraldine salt. Moreover, the shape of the electronic spectrum of polyaniline continuously changed from that typical of leucoemeraldine to that typical of emeraldine, as the potential was varied from +0.2 V to +0.93 V [72]. Thus, oxidation of the polyaniline chain results in the introduction of the fragments responsible for the charge transfer.

The correctness of assigning the electronic spectra bands of various polyaniline states is confirmed by semi-empirical [73, 74] and non-empirical [75] quantum chemical calculations of molecular orbital energies which correlate well with experimental conductivities of these polyaniline forms.

Thus, base and salt leucoemeraldine forms exhibit dielectric properties and a smaller than 10^{-8} S/cm conductivity. The emeraldine base is also a dielectric with a conductivity of 10^{-8}-10^{-13} S/cm. However, doping the emeraldine base with acids results in the emeraldine salt with a conductivity varying from 10^{-2} S/cm to 1.3 S/cm [69]. Adding to the reaction medium 20-60 wt.% of organic solvents such as ethanol, acetone, or tetrahydrofuran allows increasing the conductivity of the emeraldine salt to 10 S/cm [76], and the reaction in the dispersion system water/chloroform increases the conductivity up to 1300 S/cm [77]. Adding organic solvents that can mix with water and, particularly, that can form a separate phase, to the reaction medium, increases the conductivity of the emeraldine salt, which is attributed to the separation of the high-molecular conductive polymer from the oligomers and the monomer, whose presence is associated with the defects appearing in the chain (Scheme 6), as discussed below.

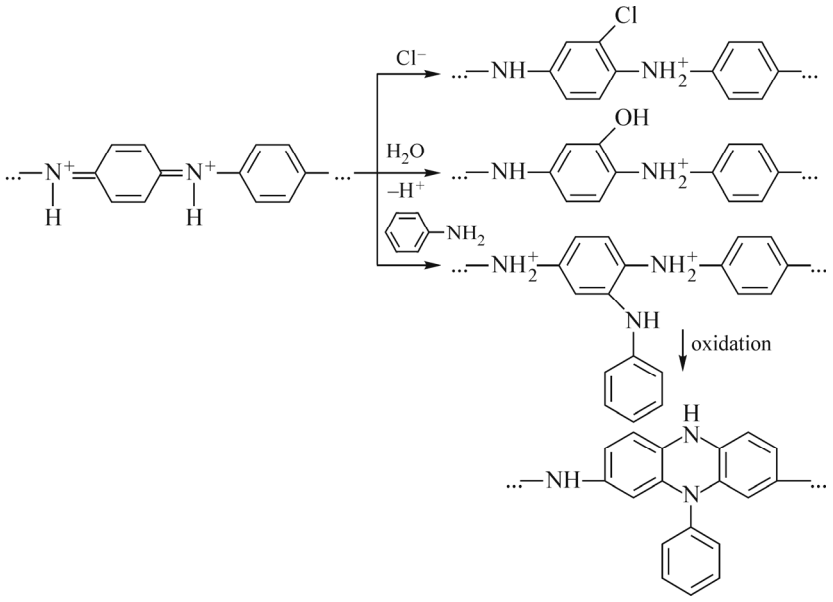

Scheme 6.

Electronic spectra of polyphenylenediamines have been much less studied, but the available data suggest that their spectra may be interpreted similarly to those of polyaniline. Thus, the electronic spectrum of poly(*o*-phenylenediamine) shows an intense absorption band with a peak at 459-465 nm, which is usually attributed to the presence of phenazine fragments in its chain (Scheme 4, I); at the same time, a band with a peak at ~270 nm attributed to aminobenzoic fragments is also sometimes reported [78-80]. The electronic spectrum of poly(*m*-phenylenediamine) shows an absorption band with a peak at 459 nm, whereas poly(*p*-phenylenediamine) exhibits absorption peaks at 405 nm and 636 nm corresponding to phenazine and quinone imine fragments. The spectrum of poly(*p*-phenylenediamine) prepared by enzymatic oxidative polymerization of *n*-phenylenediamine in the presence of horseradish peroxidase shows the bands at 308 nm, 360 nm, 543 nm assigned to the presence of other possible fragments in its chain (Scheme 4) [26, 78]. In general, the character of polyphenylenediamine spectra seems to depend largely on synthesis conditions determining the ratio of the number of highly diverse different type fragments in their chains (Scheme 4) [78-83].

Despite the cyclochain structure, poly(*p*-phenylenediamine) and poly(*o*-phenylenediamine) are soluble in N-methylpyrrolidone, N, N′-dimethylformamide, and partly in tetrahydrofuran, similar to the emeraldine base [26]. The solubility of poly(*p*-phenylenediamine) and poly(*o*-phenylenediamine) is probably due to their low number average molecular weight, which rarely exceeds 10^4, as well as to the presence of defects in their cyclochain structure. The latter fact is also considered a reason of low electrical conductivity of poly(*o*-phenylenediamine) and poly(*p*-phenylenediamine). Thus, the conductivity of poly(*p*-phenylenediamine) does not exceed $6.86 \cdot 10^{-6}$ S/cm [84] and that of poly(*o*-phenylenediamine) is still smaller and does not exceed $5.7 \cdot 10^{-7}$ S/cm in the doped state [85]. It was shown that doping of poly(*o*-phenylenediamine) significantly increases its electrical conductivity as much as $2.5 \cdot 10^{-10}$ S/cm, $3.6 \cdot 10^{-9}$ S/cm, $8.9 \cdot 10^{-8}$ S/cm, $5.7 \cdot 10^{-7}$ S/cm as the strength of the doping proton acid grows in the series CH_3COOH, $H_2C_2O_4$, H_2SO_4, $HClO_4$ [85]. Thus, low conductivity of poly(*o*-phenylenediamine) and poly(*p*-phenylenediamine) is due to low basicity of nitrogen atoms in the chain. It is also explained by the similarity between the structure of the conjugated systems of these polymers and those of pernigraniline, which is a high resistance semiconductor with a wide band gap value [81].

Poly(*m*-phenylenediamine) has a lower solubility than poly(*o*-phenylenediamine) and poly(*p*-phenylenediamine), or no solubility at all, which is explained by the presence of branching chains or even cross-linked structures [26]. At the same time, the conductivity of poly(*m*-phenylenediamine) has a quite large value of 0.064 S/cm [86].

The studies of polypyrrole electronic spectra are broadly reported [39, 87-89]. For example, the changes in the absorption band intensity of polypyrrole spectra were analyzed for the potential varying over a wide range of values [88, 89].

It was shown that the reduction of polypyrrole decreases the intensity of its long-wavelength absorption bands in the visible region, which is consistent with the fact that polypyrrole changes its color from black to pale gray as a result of dedoping [53]. In particular, it was found that the potential variation from +0.6 V to –0.6 V increases the intensity of absorption in the shortwave region associated with a simultaneous hypsochromic shift of this band, and the absorption in the longwave region is diminished [89]. In general, the spectra of highly doped polypyrrole contain a band at 340 nm assigned to the c π–π* transition, as well as the bands at 475 nm and 1240 nm corresponding to bipolarons [90]. The conductivity of polypyrrole, like that of polyaniline, is closely related to the nature of the electronic spectrum. Thus, the fully reduced polypyrrole form has a band gap of 3.2-4 eV typical of dielectrics [91, 92]. During the oxidation of the polypyrrole chain, the energy gap between the boundary orbitals is diminished to 2.5 eV, and polypyrrole becomes conductive [92]. The charge is transferred along its chain by polarons and bipolarons; however, the calculations show that the energy of formation of one bipolaron is 4.5 eV smaller than that of two polarons. Therefore, bipolarons are assumed to be the main charge carriers in the polypyrrole chain [93, 94].

The electrical conductivity of doped polypyrrole is generally higher than that of doped polyaniline and in most cases falls in the region from 1 S/cm to 100 S/cm [53]. The value of electrical conductivity of polypyrrole films is largely affected by the synthesis medium (as a rule, using electrochemical oxidative polymerization) and by the nature of the counterion. For example, the electrical conductivity of polypyrrole films obtained in the acetonitrile medium is approximately an order of magnitude larger than that of the films prepared in the aqueous medium. This fact can be explained by a shorter length of the polypyrrole chain segments participating in the conjugation during the oxidative polymerization of pyrrole in water due to the introduction of carbonyl and hydroxyl groups (defects) into the polypyrrole chain. Finally, lower synthesis temperature and orientation stretching also contribute to a more regular polypyrrole structure. Combining low-temperature polymerization of pyrrole with the orientation stretching of the resulting polypyrrole allowed obtaining films with an electrical conductivity of 3000 S/cm [53].

Although electron spectroscopy allows establishing the relationships between the energies of boundary orbitals, their electron population, and the conductivity of nitrogen-containing polyconjugated systems, vibrational spectroscopy still remains the main method to study the structure of electrically conductive polymers.

The IR spectrum of emeraldine salt exhibits a number of absorption bands most commonly assigned by original studies to the following types of vibrations [61, 95, 96]: 3434 cm^{-1} (N–H stretchings), 2923 cm^{-1} (asymmetrical C–H stretching), 2825 cm^{-1} (symmetrical C–H stretching), 1650-1620 cm^{-1} (N–H bending), 1590-1444 cm^{-1} (stretching of double bonds of quinone imine fragments and benzoic ring), 1491-1476 cm^{-1} (stretching of C=N bonds of quinone imine fragments), 1300-1200 cm^{-1} (C–N stretching), 1173-1073 cm^{-1} (in-plane bending of C–H bonds of the benzoic ring and quinone imine fragments), 908-754 cm^{-1} (out-of-plane bending of C–H bonds of the benzoic ring). The vibration spectra of phenylenediamine polymers have similar absorption bands [26, 78, 81, 97-101]; however, C=N stretchings seem to appear at slightly higher wave numbers 1570-1670 cm^{-1}, as was observed in aromatic monoamine polymers [101].

The IR spectra of polypyrrole thin films show absorption bands at 3522 cm^{-1} (N–H stretching), 1685 cm^{-1} (C=N stretching), 1558 cm^{-1} and 1487 cm^{-1} (C=C stretching), 1315 cm^{-1} (C–N stretching), 1040 cm^{-1} (in-plane vibrations of C–H bonds of the pyrrole ring), 920 cm^{-1} and 811 cm^{-1} (C–H wagging), 890 cm^{-1} (out-of-plane vibrations of C–H bonds of the pyrrole ring) [87]. These results are consistent with the data obtained by other authors [102-104]. There are also absorption bands at 2927-2814 cm^{-1} assigned to C–H stretchings of the pyrrole ring [105].

The available literature data [87, 103-106] demonstrate no clarity as far as assigning the bands to C–N and C=N stretchings. For example, C=N stretchings are assigned to the band at 1685 cm^{-1} in [87, 105] and at 1170 cm^{-1} in [104]. The assignment range is even wider for C–N stretchings [66, 77, 79, 80]. For example, C–N stretching is assigned to the bands at 1315.4 cm^{-1} in [87], 770 cm^{-1} in [105], while the authors of [103] report that the experimental wave number of the absorption band corresponding to the C–N bond is 1148 cm^{-1}, while its theoretical value calculated by the MNDO method is 1369 cm^{-1}. At the same time, it is known that the absorption due to the C–N stretching of secondary aromatic amines appears at 1350-1280 cm^{-1}, and the order of this bond is greater than unity [107]. This fact contradicts the assignment of absorption bands at

770 cm^{-1} and 1685 cm^{-1} to the CN bonds of any order. The absorption band at 770 cm^{-1} seems to be corresponding to deformation vibrations of C–H bonds, and the band at 1685 cm^{-1} results from the introduction of carbonyl groups into the chain, which are always present when polypyrrole is prepared in aqueous media.

According to the authors of this work, the very approach of interpreting the IR spectra of polypyrrole by considering C–N and C=N bonds as separate functional groups is wrong, since these groups are parts of a single π-system and have a fractional order. Moreover, when interpreting vibrational spectra of polypyrrole, the five-membered rings with different degrees of oxidation which form the chain should be considered as independent structural units, as is convincingly confirmed by the results reported in [88]. The analysis of the shape of Raman spectra depending on the potential allowed unmade it possible to identify ambiguously the most intense absorption bands in the vibrational spectra. For example, the band at 990 cm^{-1} is assigned to deformation vibrations of fully reduced (neutral) pyrrole residues in the chain. When one electron is removed (polaron formation), the geometry of the chain is distorted, the absorption band shifts to 976 cm^{-1}, and a new band at 930 cm^{-1} appears. Still further increase of the potential results in the transfer of the second electron (bipolaron formation) while the number of unoxidized pyrrole rings in the chain progressively diminishes. As a result, the signal at 990 cm^{-1} disappears and a new band occurs at 925-930 cm^{-1} corresponding to the bendings of C–H bonds of oxidized pyrrole cycles.

The bands at 1310 cm^{-1}, 1253 cm^{-1}, and 1044 cm^{-1} are assigned to the inter-ring vibrations of C–C bonds connecting rings in fully reduced polypyrrole, and the band at 1557 cm^{-1} is assigned to the stretching of pyrrole residues of fully reduced polypyrrole. The oxidized polypyrrole, whose chain is enriched with bipolarons, shows bands at 1310 cm^{-1}, 1253 cm^{-1}; however, the band at 1044 cm^{-1} characteristic of neutral polypyrrole shifts to large wave numbers (1081 cm^{-1}). At the same time, the aromaticity of pyrrole rings is broken, so that the force constants of double bonds are increased and the signal is shifted from the value of 1557 cm^{-1} characteristic of fully reduced polypyrrole to that of 1620 cm^{-1} typical of oxidized polypyrrole chains enriched with bipolarons.

The interpretation of spectral data is also significantly complicated by a number of side reactions involving the chains of conjugated aromatic polyamines. As is known, polyaniline contains 1.8 wt.% of covalent bound chlorine, significant amount of hydroxyl groups, and some number of branched chains as a result of nucleophilic conjugate addition of chloride ions (during aniline hydrochloride polymerization), water, and aniline, respectively, to electron-deficient quinone diimine fragments [108]. Considerable attention is also paid to the formation of a small number of phenazine fragments during the oxidative polymerization of aniline [56, 108-113] (Scheme 6).

According to elemental analysis and XPS data, polypyrrole chains also contain significant amounts of oxygen [53, 114-117]. At the same time, the data on oxygen-containing functional groups in the polypyrrole chain are very contradictory. According to [118], 18% of carbon atoms of the polypyrrole chain are linked to the hydroxyl group, and 4% are part of the carbonyl group. Other works report that some links of the polypyrrole chain contain simultaneously hydroxyl and carbonyl groups [119-121], while the authors of [122] assign almost all oxygen in the chain to the carbonyl group. Although the quantitative data concerning the state of oxygen in the polypyrrole chain vary considerably, there is no apparent contradiction in these results, since the introduction of oxygen into the chain is the result of a side process of its over-oxidation whose speed and selectivity obviously depend on specific conditions of pyrrole oxidative polymerization.

A special feature of polypyrrole is the cross-links between its chains formed by the bonds between α and β positions of the pyrrole ring, as is confirmed by NMR spectroscopy data [123, 124]. The presence of cross-links is also confirmed by absorption bands of polypyrrole IR spectra: their positions virtually do not depend on the oxidation level of its chain [88, 123, 125]. Also, the existence of dense cross-linking is confirmed by Monte-Carlo numerical simulations [126, 127] and XPS data [128] testifying branching occurring at every fifth link in the polypyrrole chain (Scheme 7).

Considerable attention is paid in the literature to the NMR studies of the structure of nitrogen-containing conductive and electroactive polymers. The ^{1}H NMR spectrum of emeraldine base shows a broad signal at about 7 ppm assigned to the proton of the secondary amino group, and a group of signals with chemical shifts of 7.2-7.46 ppm assigned to the proton signals of aminobenzoic and quinone diimine fragments. It is thought that the signals with chemical shifts larger than 7.4 ppm

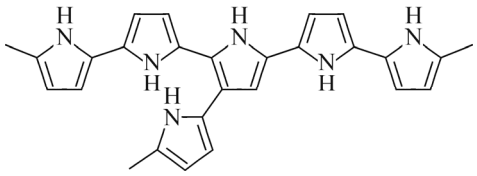

Scheme 7.

correspond to the protons of quinone imine and aminobenzoic fragments located in the *ortho* position relative to the nitrogen of the imino group. The signals with chemical shifts varying from 7.2 ppm to 7.4 ppm are assigned to the protons of aminobenzoic fragments separated from the diamagnetic-anisotropic electron-withdrawing imino groups which create a deshielding effect [129]. This assignment is also confirmed by the ^{1}H–^{1}H correlation spectroscopy (COSY) data.

In the ^{1}H NMR spectrum of the emeraldine salt, the signal of the protons bound to the nitrogen atom does not show significant broadening. This is explained by decreased exchange rate associated with three narrow equidistant signals of equal intensity with chemical shifts equal to 6.97 ppm, 7.07 ppm, and 7.17 ppm (spin-spin coupling constant is 51.1 Hz). This intensity of signals indicates a spin-spin coupling between the proton and the nitrogen atom (with the spin equal to 1), since otherwise the intensities would make a distribution approximately corresponding to Pascal's triangle coefficients [130]. Thus, the triplet in the region of 6.97-7.17 ppm corresponds to the salt groups N–H of emeraldine salt, as is evidenced by the fact that the decimal logarithm of polyaniline conductivity increases linearly from 10^{-10} S/cm to 10^{-2} S/cm with increasing integral intensity of the triplet. At the same time, the signals of the protons bound to carbon atoms virtually do not change their positions during the protonation of the emeraldine base chain [130].

Also ^{13}C NMR spectra of emeraldine base were recorded in the d^6 DMSO medium and some signals were assigned using ^{1}H–^{13}C COSY correlation spectroscopy (Scheme 8) [129].

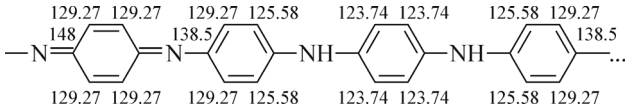

Scheme 8. Chemical shifts (ppm) in the ^{13}C NMR spectrum of emeraldine base in the d^6 DMSO medium.

Similar results were also reported in [131] for ^{13}C NMR spectra of emeraldine base recorded in the d^7 DMF medium, and weighty arguments were obtained to indicate the presence of covalently bonded chlorine atoms in the chain.

Solid phase ^{13}C NMR polyaniline spectra contain three pronounced signals in the spectrum of emeraldine base with the chemical shifts of 124.7 ppm, 144.6 ppm, and 160.3 ppm and one broad band in the emeraldine sulfate spectrum in the region of 120 ppm. The signal at 124.7 ppm is assigned to the carbon atoms bound to hydrogen atoms, and the peaks at 144.6 ppm and 160.3 ppm are assigned to the carbon atoms linked to the nitrogens of the amino and imino groups constituting the polyaniline chain [132]. Similar results were also obtained in [133].

The NMR spectra of aromatic diamines polymers have been studied much less than polyaniline polymers. The structure of poly(*o*-phenylenediamine) and poly(*p*-phenylenediamine) was investigated by ^{1}H NMR spectroscopy in d^6 DMSO solutions. The chemical shifts of the protons in secondary and primary amino groups of poly(*o*-phenylenediamine) are 4-6 ppm, and those of the protons bounded to carbon atoms are 6-8 ppm [26, 134]. In the ^{1}H NMR spectra of poly(*p*-phenylenediamine), the signals corresponding to the protons of amino groups have chemical shifts varying from 4.5 ppm to 5.8 ppm, while the protons of benzoid fragments (Scheme 4) have chemical shifts equal to 6.8 ppm, and the chemical shifts of the protons of quinone fragments (Scheme 4) fall in the region of 7.9 ppm [26, 78, 81, 101]. In general, chemical shifts, multiplicities, and signal intensities of ^{1}H NMR spectra of poly(*o*-phenylenediamine) and poly(*p*-phenylenediamine) significantly depend on their synthesis conditions, which is probably the result of a change in the ratio between the number of primary and secondary amino groups, as well as chain fragments with different oxidation levels.

The form of ^{1}H NMR spectra can be influenced by the molecular weight of phenylene diamine polymers, which usually does not exceed 10^4 and varies greatly depending on the conditions of the phenylenediamine oxidative polymerization. Also, ^{1}H NMR spectra were recorded for *m*-phenylenediamine oligomers soluble in d^6 DMSO and obtained by enzymatic oxidative polymerization under the action of horseradish peroxidase. The signals in the region of chemical shifts from 6 ppm to 8 ppm were assigned to the protons bound to carbon atoms, and the signals with a chemical shift of 4-6 ppm were assigned to the protons of the secondary amino group [26].

^{13}C NMR spectra of polyphenylenediamine were also described in literature. Poly(*o*-phenylenediamine) has peaks with the chemical shifts of 102 ppm, 126-128 ppm, and 143-145 ppm assigned to the carbon atoms bound to the hydrogen atoms of quinoid and benzoid fragments, as well as to the carbon atoms bound to the nitrogen [134]. The ^{13}C NMR spectra of poly(*p*-phenylenediamine) exhibit two groups of signals with the chemical shifts of 140 ppm, 144.9 ppm, 148.3 ppm, 153.3 ppm and 90.6 ppm, 114.3 ppm, 122.2 ppm assigned to the carbon atoms of quinoid fragments and benzoid fragments, respectively [82].

The ^{13}C NMR spectra of poly(*m*-phenylenediamine) have three signals with the chemical shifts of 117.6 ppm, 136.9 ppm, and 172.3 ppm. These signals are assigned to the atoms which 1) are bound to the hydrogen atoms of benzoid fragments, 2) belong to benzoid fragments bound to the nitrogen atoms of the secondary amino group, and 3) belong to imino groups, respectively [100].

The NMR spectra of a cross-linked polymer polypyrrole can be recorded only in the solid phase. However, there are a number of original works to interpret solid-state ^{13}C and ^{15}N NMR spectra of polypyrrole [132, 135-138].

The form of solid state ^{13}C NMR polypyrrole spectra is determined by the oxidation state of its chain. For example, the solid-state ^{13}C NMR spectrum of neutral (reduced) polypyrrole has two signals: a peak in the weak field (123 ppm) assigned to α-carbon atoms and a peak in the region of stronger fields (105 ppm) assigned to β-carbon atoms of pyrrole residues in the chain [132, 135]. On the other hand, the signals of α- and β-carbons cannot be obtained in the case of doped polypyrrole with BF_4^- counterions, so that only one broad band is observed. The chemical shifts of the signals in the solid state ^{13}C NMR spectra of polypyrrole and 2,5-dimethylpyrrole have very close values to confirm the assumption concerning preferential linking of pyrrole residues into the chains through α-positions.

^{15}N NMR spectra of polypyrrole show one broad absorption peak, which does not depend on the method of polypyrrole preparation and corresponds to the protonated nitrogen [137, 138] of both reduced and oxidized fragments, which is also confirmed by quantum chemical calculations [138].

CRYSTAL STRUCTURE OF NITROGEN-CONTAINING ELECTROCONDUCTIVE AND ELECTROACTIVE POLYMERS

Initially, electrically conductive and electroactive polymers were considered amorphous solids without a long-range three-dimensional order of their structural units; it was thought to be explained by the presence of a through conjugated system providing high thermodynamic and kinetic rigidity of the chains. However, since 1980s, a number of works have reported the presence of crystalline regions in polymers. Thus, polyconjugated systems (electrically conductive and electroactive polymers), like most other homopolymers, are partially crystalline solids.

The presence of crystalline regions is indirectly confirmed by the possibility of using the hopping conductivity model to describe the temperature dependence of electrical conductivity of doped polyaniline [139]. Thus, in the ordered regions composed of elongated regularly packed chains, the conjugation effect occurs on the longer segments of polyaniline chains, while the length of such segments is much smaller in the amorphous regions with “twisted” polyaniline chains, which leads to lower electrical conductivity. For example, a tocographic tunnelling microscopy study reported the existence of 20–80 nm domains of emeraldine salt which exhibit the same “current strength–voltage” dependencies as those observed in metals [140].

However, the decisive evidence of the presence of crystalline regions of polyaniline was obtained by X-ray diffraction. Clarifying the structure of polyaniline ordered phase is complicated by the fact that it appears in a number of various forms with different oxidation levels and degrees of protonation [141]. Polyaniline in the form of emeraldine salt and emeraldine base has two types of crystal structures. Emeraldine salt (ES), which is isolated immediately after chemical or electrochemical oxidative polymerization of aniline in acidic environment, contains ordered areas. This type of structure is referred to as ES-I. However, the emeraldine base (EB-I) obtained by treating the emeraldine salt (ES-I) with bases is amorphous. At the same time, the protonation of amorphous emeraldine base also results in the formation of partially crystalline emeraldine salt (ES-I). The formation of crystalline regions is shown by the Debye–Scherrer X-ray diffraction method during the protonation of amorphous emeraldine base (EB-I) by hydrochloric acid: the degree of crystallinity is notably increased with increasing molar ratio Cl/N as a result of doping EB with hydrochloric acid [141].

Interestingly, the degree of crystallinity of sulphate and emeraldine chloride is significantly affected by the temperature of their subsequent processing. As the temperature increases from 20 °C to 150 °C, the degree of crystallinity slightly increases; however, still further heating to 300 °C is associated with a rapid decrease in the degree of crystallinity to form almost amorphous polymer [142]. Apparently, a slight temperature increase promotes kinetic flexibility of polyaniline chains which makes a part of the segments of the emeraldine salt chain transform from the amorphous phase to the crystalline form. A further sharp decrease in the degree of crystallinity with increasing temperature is most likely due to the loss of the dopant as a result of thermal decomposition of emeraldine salts (thermal dedoping) [143]. A later work [144] devoted to the changes occurring in the structure, degree of crystallinity, and electrical conductivity of emeraldine hydrochloride under heating from 50 °C to 300°C reported that the degree of crystallinity of the sample diminished from 50% to 22% and its electrical conductivity diminished from $0.33 \cdot 10^{-4}$ S/cm to $0.4 \cdot 10^{-5}$ S/cm, which was explained both by the loss of the dopant and by cross-linking of polyaniline chains. In general, the results of the above studies are consistent, although the effect of increased degree of crystallinity under heating was not mentioned in [144], since no data were obtained by the authors about the degree of crystallinity and electrical conductivity in the temperature range from 100 °C to 200 °C.

The relationship between the degree of doping of the emeraldine base (the proportion of protonated units) and the crystallinity of the formed emeraldine salt as well as electrical conductivity is also testified by the data indicating the symbate character of these dependencies on the medium pH [142]. It was shown that the polyaniline degree of crystallinity increases from 0 (amorphous EB-I) to 23% (partially crystalline ES-I) and electrical conductivity increases from 10^{-11} S/cm to 1 S/cm as the pH decreases from 7 to 0.

If a film is made of the solution of amorphous emeraldine base (EB-I) in N-methylpyrrolidone and then the solvent is removed, the degree of crystallinity of the emeraldine base increases to about 50%. This structure of emeraldine base is referred to as EB-II. The protonation of EB-II emeraldine base with hydrochloric acid results in the formation of emeraldine salt whose ordered regions have a different structure than those of ES-I. This salt is referred to as ES-II, and its degree of crystallinity is also about 50% [141].

The following remarkable fact still remains unexplained: deprotonation of the emeraldine salt ES-II leads to the formation of the amorphous emeraldine base EB-I. The protonation of the latter, in turn, leads to the formation of the emeraldine salt with the ES-II structure rather than the expected ES-I structure [141]. Possible transitions between various polyaniline structures are shown in Scheme 9.

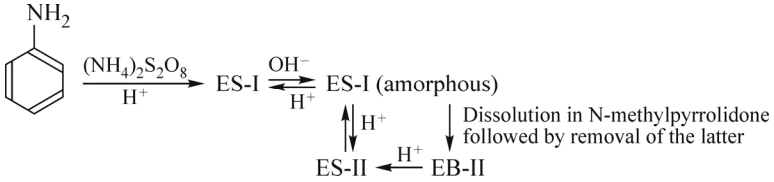

Scheme 9.

The emeraldine base EB-II has a crystallinity of ~ 50%, the size of its crystallites varying from 5 nm to 15 nm. The crystal regions have an orthorhombic lattice with the unit cell parameters a = 7.80 Å, b = 5.75 Å, c = 10.05 Å, V = 450 Å^3; the polymer chains are oriented along the direction c. Based on the lattice parameters and bond lengths C–C = 1.41 Å, C–N = 1.36 Å, C–H = 1.08 Å, the values of the bond angle C–NH–C and the angle between the planes containing the neighboring rings were estimated to be 136±5° and 30°, respectively. Thus, benzoic rings of the emeraldine base are non-coplanar, which is consistent with its very low electrical conductivity. Note that bond lengths were obtained using X-ray diffraction for aniline tetramer single crystals [145], and the calculations in [141] were carried out neglecting the difference between the bond lengths of aminobenzoic and quinone imine fragments.

A characteristic feature of emeraldine base fibers and films is a substantial increase in crystallinity during the orientation due to the formation of new crystallites [146]. Thus, with the draw ratio of 3.5, the crystallinity of emeraldine base increases from 11-15% to 20-30% [147], and still further increase of the draw ratio to 4.5 causes the orientation effect also in the amorphous phase, which acquires a nematic liquid crystal structure [146].

The emeraldine salt ES-II formed by the protonation of the emeraldine base EB-II also has an orthorhombic lattice characterized by unit cell parameters a = 7.0 Å, b = 8.6 Å, c = 10.4 Å, V = 620 Å^3; however, according to the calculation, the dihedral angle θ between benzoic rings is decreased to form nearly coplanar arrangement of the rings in the chain and agrees with the fact that electrical conductivity increases up to ten orders of magnitude when passing from the emeraldine base to the emeraldine salt. The formation of the ES-II structure by doping EB-II can be represented as a result of the middle chain in the EB-II unit cell being shifted by b/2 and c/2 and by the introduction of dopant ions between the layers (a, c) [141].

The structure of ordered regions of the emeraldine salt ES-I formed directly during the oxidative polymerization of aniline was established in [141] with a lower certainty. It is assumed that the lattice is also orthorhombic with the unit cell parameters a = 4.3 v, b = 5.9 Å, c = 9.6 Å, V = 245 Å^3. The ES-I unit cell volume is slightly smaller than that of the repeated fragment of the EB-II base chain (225 Å^3); the difference between their volumes is 20 Å^3, which is close to the volume of the Cl^- ion (25 Å^3). Thus, the ES-I unit cell contains only one polymer zigzag and one Cl^- anion. The bond angle C–NH–C is about 120°, and the dihedral angle between the planes containing adjacent rings varies from 0° to 15°.

The authors of the classical work [141] in the field of structural chemistry of polyconjugated systems expressed their doubts regarding the lattice type and the unit cell parameters of emeraldine salt (ES-I), which stimulated the research in this field. The unit cell parameters a = 5.7 Å, b = 17.8 Å, c = 22.8 Å, α = 83.1575°, β = 84.6971°, γ = 88.4419° were obtained in a later work [147] devoted to the determination of the structure of ordered regions using X-ray diffraction for emeraldine chloride (ES-I) obtained by oxidative polymerization of aniline in hydrochloric acid aqueous solution under the action of ammonium peroxydisulfate used as an oxidizing agent. It was shown that the structure of the ordered regions of emeraldine hydrochloride does not change with time under the synthesis conditions.

Numerous studies of the influence of the nature of the dopant anion on the interplanar distance in the ordered regions of various emeraldine salts are also worth mentioning. It was established that the increase of the size of the dopant ion in the $Cl^- < ClO_4^- <$ n-toluene sulfonate series is expectedly associated with the increase of interplanar distances up to 0.4 nm, 0.7 nm, and 1.4 nm, respectively, which is consistent with molecular mechanics calculations [148]. It is noteworthy that doping amorphous emeraldine base with various acids results in the formation of the ES-I structure whose crystallinity increases with increasing size of dopant counterions, e.g., in the series from p-toluenesulfonic anions and 5-sulfosalicylic acid to the anions of camphor sulphate and dodecylbenzenesulfonate [149, 150]. High crystallinity of emeraldine salt doped with acids with large hydrophobic anions can be explained by the fact that they are more densely and regularly packed in the interchain space due to hydrophobic interactions [151, 152]. The effect of crystallinity increase in the emeraldine salt is usually observed at low doping levels by acids with large anions (dopant/aniline molar ratio is ≈0.2); however, the crystallinity diminishes significantly as the level of doping increases due to the destruction of the ordered structure by large anions of the dopant [153].

The structure of ordered regions was also studied for some polyaniline derivatives. For example, the crystalline ordering of three polymers poly(*m*-aminophenol), polyaniline, and poly(*m*-aminobenzoic acid) obtained under identical conditions was compared [154]. The crystallinity was found to increase in the series poly(*m*-nitroaniline) (25%)<polyaniline (45%)<poly(*m*-aminophenol) (60%). Lower crystallinity of poly(*m*-nitroaniline) compared to that of polyaniline correlates with the presence of a nitro group which can participate in the formation of intramolecular hydrogen bonding to suppress interchain interactions, which lead to the formation of ordered regions. On the contrary, higher crystallinity of poly(*m*-aminophenol) compared to that of polyaniline can be explained by the ability of phenolic hydroxyl groups to form intermolecular hydrogen bonds associated with stronger interchain interactions.

The structure of crystalline regions of poly(2-methoxyaniline) hydrochloride was also studied [155]. It was shown that the increase of synthesis time from 0.5 h to 72 h make the degree of crystallinity of poly(2-methoxyaniline) hydrochloride increase from 48% to 63% due to acid-catalyzed oxidative degradation of poly(2-methoxyaniline) [11] occurring mainly in amorphous regions. On the other hand, the basic form of emeraldine salt of poly(2-methoxyaniline) is formed when the latter is neutralized by aqueous solution of sodium hydroxide. This form exhibits substantial crystallinity, in contrast to the emeraldine polyaniline base obtained by the treatment with bases isolated directly after the oxidative polymerization of emeraldine salts of polyaniline. This can be explained by the formation of interchain hydrogen bonds between the methoxy group and the secondary amino group of poly(2-methoxyaniline) which promotes the ordering. It was also established that the degree of crystallinity of the resulting emeraldine base diminishes from 38% to 27%, as the time of neutralization with sodium hydroxide increases. This effect is thought to be possibly caused by the development of alkaline hydrolytic degradation of poly(2-methoxaniline) chains. Note that emeraldine salt (a = 7.0073 Å, b = 10.6078 Å, c = 22.5234 Å, α = 83.3783°, β = 84.7231°, γ = 89.0455°) and the salt (a = 6.793 Å, b = 9.529 Å, c = 19.640 Å, α = 83.043°, β = 84.656°, γ = 88.586°) of poly(2-methoxaniline) have similar unit cell parameters to indicate the stabilization of the emeraldine base structure, probably due to the inclusion of hydroxide ions into ordered the regions [155].

It was established that the degree of crystallinity decreases with increasing size of the substituents in the emeraldine base chain. Thus, the degree of crystallinity of poly(2-ethoxyaniline) emeraldine salt is about 39%, which is significantly lower than that observed for the poly(2-methoxyaniline) emeraldine salt [156].

The expected structure of ordered regions of the leucoemeraldine form of polyaniline was studied using a model oligomer (N-phenyl-capped tetraaniline) which forms crystals with a monoclinic lattice and unit cell parameters a = 13.93 Å, b = 8.82 Å, c = 23.2 Å, β = 95.038° [157].

Unlike aniline polymers, phenylenediamine polymers are usually almost amorphous or exhibit a small degree of crystallinity. This is explained by the fact that the number of possible structures of their chain fragments is too large to form any regular supramolecular structures. Note also that the degree of crystallinity of polyphenylenediamines is small and decreases in the series poly(*p*-phenylenediamine)>poly(*o*-phenylenediamine)>poly(*m*-phenylenediamine) due to the increased diversity of polymer chain fragments when passing from poly(*p*-phenylenediamine) to poly(*m*-phenylenediamine). Single cases of phenylenediamine oxidation products exhibiting significant crystallinity [26] are probably explained by the realization of conditions when some types of chain fragments are significantly more numerous than other types (Scheme 4). Possibly, the conditions of high selectivity of oxidative polymerization with respect to certain types of chain fragments will be found as polyphenylenediamine synthesis methods will be further elaborated to obtain polymers with a high degree of crystallinity.

The structure of polypyrrole crystalline regions was studied mainly on the samples obtained by electrochemical oxidative polymerization of pyrrole in the presence of various dopants. Thus, polypyrrole prepared by electrochemical oxidative polymerization of pyrrole in the presence of *n*-toluenesulfonic acid showed significant molecular anisotropy [158, 159]. This fact is explained by the *trans*-coordination of pyrrole rings inside polypyrrole chains: the rings lie in the planes parallel to the electrode surface but are randomly oriented in the direction perpendicular to the electrode surface. According to other studies, the anisotropy is characteristic only of polypyrrole doped with planar counterions, whereas doping with non-planar anions such as tetrafluoroborate, sulfate, and perchlorate results in the isotropic layer being formed

on the electrode surfaces [160, 161]. It was established that the degree of anisotropy of polypyrrole films remaining on the electrode surface is increased substantially with decreasing temperature, increasing dopant/monomer molar ratio, and increasing anodic potential, as well as during mechanical stretching [159, 162-164]. At the same time, the increase of molecular anisotropy is in all cases associated with increased electrical conductivity, which is probably due to the increased length of conjugated chain segments.

The structure of crystalline regions of electrochemically prepared polypyrrole with a PF_6^- counterion was studied in most detail. It was established that the degree of crystallinity and electrical conductivity simultaneously increase with decreasing temperature and current density. It was shown that electrical conductivity of polypyrrole is increased from 100 S/cm to 300 S/cm as the temperature decreases from 20 °C to –40 °C during the electrochemical polymerization of pyrrole, and electrical conductivity increases from 50 S/cm to 300 S/cm as the current density diminishes from 1 мA/cm^2 to 0.05 мA/cm^2. The ordered regions of polypyrrole doped with PF_6^- anions have a monoclinic crystal lattice [165]. Interestingly, the degree of crystallinity reaches maximum when passing from the extremely oxidized polypyrrole with PF_6^- counterions to the fully reduced polypyrrole as the potential diminishes [166].

The dopant counterions seem to be evenly distributed between the layers of polypyrrole chains [166] so that the formation of ordered structures requires a balance of electrostatic repulsion between positively charged segments of polypyrrole chains and negatively charged dopant ions distributed over the interchain space, as well as a balance of attraction forces between the segments of polypyrrole chains and the dopant ions.

Even though a vast majority of works concerns the monoclinic crystal lattice with transoid junction of pyrrole cycles, the most interesting results were obtained when studying the products of pyrrole electropolymerization in the presence of sodium dodecyl sulfate [167]. According to electron and X-ray diffraction data, polypyrrole doped with dodecyl sulfate ions has a hexagonal structure with a cisoid junction of pyrrole cycles. The observed structure also appears in the polymer bulk, although with a smaller crystallinity than that of thin films on the electrode surface.

Thus, the percentage of polypyrrole crystallinity is very sensitive to almost all variations of synthesis parameters, so that the careful control over the conditions of electrochemical oxidative polymerization of pyrrole allows obtaining films with a high degree of crystallinity up to 68% [168].

CONCLUSIONS

Nitrogen-containing electrically conductive and electroactive polymers appear in a number of states with different degrees of protonation, contents of oxidized fragments, and (in the case of phenylenediamine polymers) different content of condensed heterocycles in the chain. A fundamental property of electrically conductive polymers is the multiplicity of their forms corresponding to the products of oxidative polymerization of the same monomer, so that these forms continuously transform into each other under the variation of the potential and the pH of the reaction system. The changes in their electronic and crystal structures depending on the synthesis conditions makes spectral methods special as far as identifying each state to be realized. In this regard, the systematic analysis of literature data on electron, vibrational, and NMR spectroscopy of nitrogen-containing polyconjugated systems presented in this review is of considerable interest. The relationship between the nature of absorption, the position of protolytic and redox equilibria in the system, the geometry of the unit cell, and the electrical conductivity of nitrogen-containing electrically conductive and electroactive polymers has been established.

FUNDING

This work was financially supported by the Mendeleev University of Chemical Technology of Russia, project No. 006-2018.

CONFLICT OF INTERESTS

The authors declare that they have no conflict of interests.

REFERENCES

1. G. G. Wallace, G. M. Spinks, L. A. P. Kane-Maguire, and P. R. Teasdale. Conductive Electroactive Polymers. CRC Press: N.Y., **2003**.
2. B. Wessling. *Chem. Innovation*, **2001**, *31*, 34.
3. H. S. O. Chan, P. K. H. Ho, E. Khor, M. M. Tan, K. L. Tan, B. T. G. Tan, and Y. K. Lim. *Synth. Met*., **1989**, *31*, 95.
4. A. A. Matnishyan, T. L. Akhnazaryan, G. V. Abagyan, G. R. Badalyan, S. I. Petrosyan, and V. D. Kravtsova. *Phys. Solid State*, **2011**, *53*, 1727.
5. M. Rashid and S. Sabir. *Orient. J. Chem*., **2008**, *24*, 129.
6. O. Melad and M. Hilles. *Bio. Chem. Res*., **2015**, 75.
7. H. Minami, M. Okubo, K. Murakami, and S. Hirano. *J. Polym. Sci*., *Part A*, **2000**, *38*, 4238.
8. Vasant Chabukswar and Ganesh Sable. *Chem. Chemic. Technol*., **2009**, *3*, 95.
9. A. D. Borkar. *Int. J. Chem. Phys. Sci.*, **2014**, *3*(4), 80–85.
10. I. Mav and M. Zigon. *J. Polym. Sci*., **2001**, *39*, 2471.
11. Ya. O. Mezhuev, Yu. V. Korshak, M. I. Shtilman, S. P. Brudz, S. E. Pokhil, A. A. Firer, and I. S. Strakhov. *Int. Polym. Sci. Technol*., **2015**, *42*, T21.
12. I. Mav and M. Zigon. *J. Polym. Sci*., **2001**, *39*, 2482.
13. R. Suresh, K. Giribabu, R. Manigandan, L. Vijayalakshmi, A. Stephen, and V. Narayanan. *Chem. Sci. Trans*., **2013**, *2*(S1), S202.
14. A. R. Ando, G. M. do Nascimento, R. Landers, and P. S. Santos. *Spectrochim. Acta*, *Part A*, **2008**, *69*, 319.
15. S. Z. Ozkan, I. S. Eremeev, G. P. Karpacheva, and G. N. Bondarenko. *Open J. Polym. Chem*., **2013**, *3*, 63.
16. Ya. O. Mezhuev, Yu. V. Korshak, M. I. Shtilman, and I. S. Strakhov. *Theor. Experiment. Chem*., **2014**, *50*, 331.
17. S. M. Sayyah and S. M. Mohamed. *J. Appl. Chem*., **2015**, *8*, 28.
18. E. Lapin, I. Jureviciute, R. Mazeikiene, G. Niaura, and A. Malinauskas. *Synth. Met*., **2010**, *160*, 1843.
19. Ya. O. Mezhuev, Yu. V. Korshak, M. I. Shtilman, S. E. Pokhil, and I. S. Strakhov. *Russ. J. Gen. Chem*., **2015**, *85*, 1482.
20. X-G. Li, M-R. Huang, Yi Jin, and Yu-Liang Yang. *Polymer*, **2001**, *42*, 3427.
21. J. Stejskal. *Prog. Polymer Sci*., **2015**, *41*, 1.
22. M-R. Huang, X-G. Li, and Y. Yang. *Polym. Degrad. Stab*., **2001**, *71*, 31.
23. I. Amer, D. A. Young, and H. C. M. Vosloo. *Eur. Polym. J*., **2013**, *49*, 3251.
24. A. Janosevic, B. Marjanovic, A. Rakic, and G. Ciric-Marjanovic. *J. Serb. Chem. Soc*., **2010**, *75*, 1181.
25. I. S. Strakhov, Ya. O. Mezhuev, Yu. V. Korshak, and M. I. Shtilman. *Russ. J. Gen. Chem*., **2016**, *86*, 2682.
26. X-G. Li, M-R. Huang, W. Duan, and Y-L. Yang. *Chem. Rev*., **2002**, *102*, 2925.
27. S. M. Sayyah, M. M. El-Deeb, S. M. Kamal, and R. E. Azooz. *J. Appl. Polym. Sci*., **2009**, *112*, 3695.
28. E. M. Genies, G. Bidan, and A. F. Diaz. *J. Electroanal. Chem*., **1983**, *149*, 101.
29. S. Sadki, P. Schottland, N. Brodie, and S. Sabouraud. *Chem. Soc. Rev*., **2000**, *29*, 289.
30. C. P. Andrieux, P. Audebert, P. Hapiot, and J. M. Saveant. *J. Phys. Chem*., **1991**, *95*, 10158.
31. P. S. Sargin, L. Toppare, and E. Yurtsever. *Polymer*, **1996**, *37*, 1151.
32. S. Cavallaro, A. Colligiani, and G. Cum. *J. Thermal. Anal*., **1992**, *38*, 2649.
33. R. B. Bjorklund. *J. Chem. Soc*., *Faraday Trans.*, *1*, **1987**, *83*, 1507.
34. S. Bhadra. *Prog. Polym. Sci*., **2009**, *34*, 783.
35. T. Hagivara, T. Demura, and K. Iwata. *Synth. Met*., **1987**, *18*, 317.

36. A. G. MacDiarmid. *Synth. Met*., **2001**, *125*, 11.
37. G. Nesher, G. Marom, and D. Avnir. *Chem. Mater*., **2008**, *20*, 4425.
38. P. Chowdhury and B. Saha. *Ind. J. Chem. Technol*., **2005**, *12*, 671.
39. A. Malinauskas. *Polymer*, **2001**, *42*, 3957.
40. A. A. Syed and M. K. Dinesan. *Talanta*, **1991**, *38*, 815.
41. S. Picart, F. Miomandre, and V. Launay. *Bull. de l'Union des Physiciens*, **2001**, *95*, 581.
42. R. Cruz-Silva, J. Romero-Garcıa, J. L. Angulo-Sanchez, A. Ledezma-Perez, E. Arias-Marın, and I. Moggio. *Eur. Polym. J*., **2005**, *41*, 1129–1135.
43. G. V. Otrokhov, O. V. Morozova, I. S. Vasil′eva, G. P. Shumakovich, E. A. Zaitseva, M. E. Khlupova, and A. I. Yaropolov. *Biochemistry*, **2013**, *78*, 1539.
44. A. Roberts, R. Gill, R. J. Hussey, H. Mikolajek, P. T. Erskine, J. B. Coope, S. P. Wood, E. J. Chrystal, and P. M. Shoolingin-Jordan. *Acta Crystallogr. D. Biol Crystallogr.*, **2013**, *69*, 471.
45. R. Catranescu, I. Bobirnac, M. Crisan, A. Cojocaru, and I. Maior. *U.P.B. Sci. Bull*., *Series B*., **2012**, *74*, 49.
46. Y. Wei, X. Tang, and Y. Sun. *J. Polym. Sci*., *Part A*., **1989**, *27*, 2385.
47. J. Nie, D. E. Tallman, and G. P. Bierwagen. *J. Coat. Technol. Res*., **2008**, *5*, 327.
48. Y. Wei, Y. Sun, and X. Tang. *J. Phys. Chem*., **1989**, *93*, 4878.
49. K. Liu, Z. Hu, R. Xue, J. Zhang, and J. Zhu. *J. Power Sources*, **2008**, *179*, 858.
50. A. Malinauskas and J. Malinauskiene. *Chemija*, **2005**, *16*(1), 1.
51. W. W. Focke, G. E. Wnek, and Y. Wei. *J. Phys. Chem*., **2009**, *91*, 5813.
52. J. Stejskal, P. Kratochvil, and A. D. Jenkins. *Polymer*, **1996**, *37*, 367.
53. T. V. Vernitskaya and O. N. Efimov. *Russ. Chem. Rev*., **1997**, *66*, 443.
54. J. Stejskal, P. Kratochvil, and A. D. Jenkins. *Collect. Czech. Chem. Commun*., **1995**, *60*, 1774.
55. W. S. Huang, A. G. MacDiarmid, and A. J. Epstein. *J. Chem. Soc*., *Chem. Commun*., **1987**, 1784.
56. I. Yu. Sapurina and J. Stejskal. *Russ. Chem. Rev*., **2010**, *79*, 1123.
57. A. J. Epstein, J. M. Ginder, F. Zuo, H.-S. Woo, D. B. Tanner, A. F. Richter, M. Angelopoulos, W.-S. Huang, and A. G. MacDiarmid. *Synth. Met*., **1987**, *21*(1-3), 63.
58. M. Trchová, Z. Morávková, I. Šeděnková, and J. Stejskal. *Chem. Pap.*, **2012**, *66*(5), 415.
59. I. S. Strakhov, Ya. O. Mezhuev, Yu. V. Korshak, A. L. Kovarskii, and M. I. Shtil′man. *Russ. J. Appl. Chem*., **2016**, *89*(3), 447.
60. I. S. Strakhov, A. I. Rodnaya, Ya. O. Mezhuev, Yu. V. Korshak, and T. A. Vagramyan. *Russ. J. Appl. Chem*., **2014**, *87*(12), 1918.
61. B. Kavitha, K. Prabakar, K. Siva kumar, D. Srinivasu, Ch. Srinivas, V. K. Aswal, V. Siriguri, and N. Narsimlu. *IOSR J. Appl. Chem*., **2012**, *2*, 16.
62. M. Angelopoulos, G. E. Asturias, S. P. Ermer, A. Ray, E. M. Scherr, A. G. Macdiarmid, M. Akhtar, Z. Kiss, and A. J. Epstein. *Mol. Cryst. Liq. Cryst. Inc. Nonlin. Opt*., **1988**, *160*(1), 151.
63. F. Yılmaz and Z. Küçükyavuz. *Polym. Int*., **2010**, *59*(4), 552.
64. M. Angelopoulos, R. Dipietro, W. G. Zheng, A. G. MacDiarmid, and A. J. Epstein. *Synth. Met*., **1997**, *84*, 35.
65. D. Yang, P. N. Adams, and B. R. Mattes. *Synth. Met*., **2001**, *119*, 301.
66. Ya. O. Mezhuev, Yu. V. Korshak, and M. I. Shtilman. *Russ. Chem. Rev.,* **2017**, *86*(12), 1271.
67. Ya. O. Mezhuev, Yu. V. Korshak, and M. I. Shtil′man. *Russ. J. Gen. Chem*., **2016**, *86*(11), 2520.
68. Ya. O. Mezhuev, Yu. V. Korshak, and M. I. Shtilman. *Russ. J. Phys. Chem. B*., **2015**, *9*(2), 306.
69. Ya. O. Mezhuev, Yu. V. Korshak, M. I. Shtilman, and I. V. Solovyova. *Russ. J. Gen. Chem*., **2014**, *84*(12), 2445.
70. K. M. Molapo, P. M. Ndangili, R. F. Ajayi, G. Mbambisa, S. M. Mailu, N. Njomo, M. Masikini, P. Baker, and E. I. Iwuoha. *Int. J. Electrochem. Sci*., **2012**, *7*, 11859.
71. M. Wan. *J. Polym. Sci*., *Part A*, **1992**, *30*, 543.

72. W. S. Huang and A. G. MacDiarmid. *Polymer*, **1993**, *34*, 1833.
73. J. Libert, J. Cornil, D. A. dos Santos, and J. L. Brédas. *Phys. Rev. B*., **1997**, *56*, 8638.
74. Z. T. de Oliveira and M. C. dos Santos. *Chem. Phys*., **2000**, *260*, 95.
75. S. A. Jansen, T. Duong, A. Major, Y. Wei, and L. T. Sein. *Synth. Met*., **1999**, *105*, 107.
76. Y. Geng, J. Li, Z. Sun, X. Jing, and F. Wang. *Synth. Met*., **1998**, *96*, 1.
77. K. Lee, S. Cho, S. H. Park, A. J. Heeger, C.-W. Lee, and S.-H. Lee. *Nature*, **2006**, *441*, 65.
78. D. Ichinohe, T. Muranaka, T. Sasaki, M. Kobayashi, and H. Kise. *J. Polym. Sci*., *Part A: Polym. Chem*., **1998**, *36*, 2593.
79. Q. H. Wu, X. Y. Xiao, Y. Y. Yang, L. R. Cai, H. P. Dai, and S. G. Sun. *Chin. J. Appl. Chem*., **1999**, *16*, 5.
80. K. Ogura, H. Shiigi, and M. Nakayama. *J. Electrochem. Soc*., **1996**, *143*, 2925.
81. F. Cataldo. *Eur. Polym. J*., **1996**, *32*, 43.
82. A. Puzari and J. B. Baruah. *React. Funct. Polym*., **2001**, *47*, 147.
83. A. H. Premasiri and W. B. Euler. *Macromol. Chem. Phys*., **1995**, *196*, 3655.
84. B. Rawat, S. S. Kansara, and H. S. Rama. *Polym. Int*., **1991**, *26*, 233.
85. H. S. O. Chan, S. C. Ng, T. S. A. Hor, J. Sun, K. L. Tan, and B. T. G. Tan. *Eur. Polym. J*., **1991**, *27*, 1303.
86. B. M. Prasad, D. Singh, and R. A. Misra, *J. Polym. Mater*., **1996**, *13*(2), 157.
87. M. A. Chougule, S. G. Pawara, P. R. Godsea, R. N. Mulika, S. Senb, and V. B. Patila. *Soft Nanosci. Lett*., **2011**, *1*, 6.
88. M. J. L. Santos, A. G. Brolo, and E. M. Girotto. *Electrochim. Acta*, **2007**, *52*, 6141.
89. A. Kêpas, M. Grzeszczuk, C. Kvarnström, T. Lindforand, and A. Ivaska. *Polish J. Chem*., **2007**, *81*, 2207.
90. Y. Hu, R. Yang, D. F. Evans, and J. H. Weaver. *Phys. Rev. B*, **1991**, *44*, 13660.
91. J. L. Bredas, and G. B. Street. *Acc. Chem. Res.*, **1985**, *18*, 309.
92. J. L. Bredas. In: Handbook of Conducting Polymers. Vol. 2. (Ed. T.A. Skotheim). Marcel Dekker: New York, Basel, **1986**, 859.
93. J. L. Bredas, B. Themans, J. M. Andre, R. R. Chance, and R. Silbey. *Synth. Met*., **1984**, *9*, 265.
94. F. Genoud, M. Guglielmi, M. Nechtschein, E. Genies, and M. Salmon. *Phys. Rev. Lett*., **1985**, *55*, *118*, 136.
95. M. Trchová and J. Stejskal. *Pure Appl. Chem*., **2011**, *83*, 1803.
96. J. Vivekanandan, V. Ponnusamy, A. Mahudeswaran, and P. S. Vijayanand. *Arch. Appl. Sci. Res*., **2011**, *3*, 147.
97. Ya. O. Mezhuev, Yu. V. Korshak, M. I. Shtilman, S. V. Osadchenko, and M. A. Salop. *Int. Polym. Sci. Tech*., **2013**, *40*, T25.
98. D. Ichinohe, T. Muranaka, and H. Kise. *J. Appl. Polym. Sci*., **1998**, *70*, 717.
99. M.-R. Huang, X.-G. Li, and Y.-L.Yang. *Polym. Degrad. Stabil*., **2001**, *71*, 31.
100. X-G. Li, W. Duan, M. R. Huang, and Y. L. Yang. *J. Polym. Sci*., *Part A: Polym. Chem*., **2001**, *39*, 3989.
101. X.-G. Li, M.-R. Huang, R.-F. Chen, Y. Jin, and Y.-L. Yang. *J. Appl. Polym. Sci*., **2001**, *81*, 3107.
102. H. J. Kharat, K. P. Kakade, P. A. Savale, K. Dutta, P. Ghosh, and M. D. Shirsat. *Polym. Adv. Technol.*, **2007**, *18*, 397.
103. B. Tian and G. Zerbi. *J. Chem. Phys*., **2009**, *92*, 3886.
104. K. Arora, A. Chaubey, R. Singhal, R. P. Singh, M. K. Pandey, S. B. Samanta., B. D. Malhotra, and S. Chand. *Biosens. Bioelectron.*, **2006**, *21*, 1777.
105. H. M. B. Darwish and S. Okur. *Am. J. Nanosci*., **2017**, *3*, 1.
106. K. Khati, I. Joshi, A. Bisht, and M. G. H. Zaidi. *IOSR J. Appl. Chem*., **2016**, *9*, 42.
107. R. M. Silverstein, F. X. Webster, and D. J. Kiemle. Spectrometric Identification of Organic Compounds. John Wiley & Sons, Inc.: New Jersey, USA, **2005**.
108. A. A. Matneyshyan, T. L. Akhnazaryan, and T. T. Khachatryan. Chem. J. of Armenia, 2013, 66, 495.
109. Y. F. Huang and C. W. Lin. *Polymer*, **2009**, *50*, 775.
110. J. Stejskal, I. Sapurina, M. Trchova, and E. N. Konyushenko, P. Holler. *Polymer*, **2006**, *47*, 8253.
111. X. X. Liu, L. Zhang, Y-B. Li, L-J. Bian, Y-Q. Hio, and Z. Su. *Polym. Bull*., **2006**, *57*, 825.
112. R. Mathew, D. Yang, B. R. Mattes, and M. P. Espe. *Macromol*., **2002**, *35*, 7575.

113. L. Ding, X. Wang, and R. V. Gregory. *Synth. Met*., **1999**, *104*, 73.
114. J. P. Pouget, Z. Oblakowski, Y. Nogami, P. A. Albouy, M. Laridjani, E. J. Oh, Y. Min, A. G. MacDiarmid, J. Tsukamoto, T. Ishiguro, and A. J. Epstein. *Synth. Met*., **1994**, *65*, 131.
115. A. F. Diaz, J. I. Castillo, J. A. Logan, and W-Y. Lee. *J. Electroanal. Chem*., **1981**, *129*, 115.
116. A. F. Diaz and K. K. Kanazawa. CRC Press: New York, **1983**, 417.
117. A. Nani, I. Craciunescu, A. Bende, R. Turcu, D. Reichert, and J. Liebscher. *Nanostruct. Polymers Nanocompos.*, **2008**, *4*(1), 3.
118. J. Mansouri and R. P. Burford. *Polymer*, **1997**, *38*, 6055.
119. S. L. Hawkins and N. M. Ratcliffe. *J. Mat. Chem*., **2000**, *10*, 2057.
120. E. T. Kang, K. G. Neoh, Y. K. Ong, K. L. Tan, and B. T-G.Tan. *Macromol*., **1991**, *24*, 2822.
121. J. Lei, C. R. Martin. *Synth. Met*., **1992**, *48*, 331.
122. P. Novak. *Electrochim. Acta*., **1992**, *37*, 1227.
123. J. N. Barisci, G. Harper, A. J. Hodgson, L. Liu, and G. G. Wallace. *React. Funct. Poly*., **1999**, *39*, 269.
124. J. M. Ribo, A. Dicko, M. A. Valles, J. Claret, P. Daliemer, N. Ferrer-Anglada, R. Bonnett, and D. Bloor. *Polymer*, **1993**, *34*, 1047.
125. R. G. Davidson and T. G. Turner. *Synth. Met*., **1995**, *72*, 121.
126. E. Yurtsever, O. Esenturk, H. O. Pamuk, and M. Yurtsever. *Synth. Met*., **1999**, *98*, 229.
127. E. Yurtsever and M. A.Yurtsever. *Synth. Met*., **1999**, *101*, 335.
128. J. Joo, J. K. Lee, J. S. Baeck, K. H. Kim, E. J. Oh, and J. Epstein. *Synth. Met*., **2001**, *117*, 45.
129. N. Naar, S. Lamouri, I. Jeacomine, A. Pron, and M. Rinaudo. *J. Macromol. Sci*., *Part A*, **2012**, *49*, 897.
130. X. Wang, T. Sun, C. Wang, W. Zhang, and Y. Wei. *Macromol. Chem. Phys*., **2010**, *211*, 1814.
131. S. Ni, J. Tang, F. Wang, and L. Shen. *Polymer*, **1992**, *33*, 3607.
132. F. Devreux, G. Bidan, A. A. Syed, and C. Tsintavis. *J. Phys.*, **1985**, *46*, 1595.
133. Z. D. Zujovic, M. Gizdavic-Nikolaidis, and G. A. Bowmaker. *Chem.*, **2013**, *77*, 87.
134. S. Kobayashi, I. Kaneko, and H. Uyama. *Chem. Lett*., **1992**, *243*, 393.
135. M. Forsyth, V-T. Truong, and M. E. Smith. *Polymer*, **1994**, *35*, 1593.
136. M. Forsyth and V-T. Truong. *Polymer*, **1995**, *36*, 725.
137. M. Kikuchi, H. Kurosu, and I. Ando. *J. Mol. Struct*., **1992**, *269*, 183.
138. B. Wehrle, H. H. Limbach, J. Mortensen, and J. Heinze. *Synth. Metals*, **1990**, *38*, 293.
139. F. Zuo, M. Angelopoulos, A. G. MacDiarmid, and A. J. Epstein. *Phys. Rev*., *B: Condens. Matter*., **1989**, *39*, 3570.
140. S. T. Yau, J. N. Barisci, and G. M. Spinks. *Appl. Phys. Lett*., **1999**, *74*, 667.
141. J. P. Pouget, M. E. Jozefowicz, A. J. Epstein, X. Tang, and A. G. MacDiarmid. *Macromolecules*, **1991**, *24*, 779.
142. W. Fosong, T. Jinsong, W. Lixiang, Z. Hongfang, and M. Zhishen. *Mol. Cryst. Liq. Cryst. Incorp. Nonlin. Opt.*, **1988**, *160*, 175–184.
143. R. Ansari and M. B. Keivani. *E-J. Chem.*, **2006**, *3*, 202.
144. L. R. de Oliveira, L. Manzato, Y. P. Mascarenhas, and E. A. Sanches. *J. Mol. Struct.*, **2017**, *15*, 707.
145. R.H. Baughman, J.F. Wolf, H. Eckhardt, L.W. Shacklette. *Synth. Met.* **1988**, *25*, 121.
146. J. E. Fischer, X. Tang, E. M. Scherr, V. B. Cajipe, and A. G. MacDiarmid. *Synth. Met*., **1991**, *41*, 661.
147. E.A. Sanches, J.C. Soares, A.C. Mafud, E.G.R. Fernandes, F.L. Leite, Y.P. Mascarenhas. *J. Mol. Struct*., **2013**, *1036*, 121.
148. C. Zhu, C. Wang, L. Yang, C. Bai, and F. Wang. *Appl. Phys. A: Mater. Sci. Process*., **1999**, *68*, 435.
149. D. Yang, P. N. Adams, and B. R. Mattes. *Synth. Met*., **2001**, *119*, 301.
150. S. Saravanan, C. J. Mathai, M. R. Anantharaman, S. Venkatachalam, and P. V. Prabhakaran. *J. Pys. Chem. Solids*, **2006**, *67*, 1496.
151. B. Dufour, P. Rannou, P. Fedorko, D. Djurado, J.-P. Travers, and A. Pron. *Chem. Mat*., **2001**, *13*, 4032.

152. K. Levon, K. H. Ho, W. Y. Zheng, J. Laakso, T. Karna, T. Taka, and J. E Osterholm. *Polymer*, **1995**, *36*, 2733.
153. J. Laska, D. Djurado, and W. Lunzy. *Eur. Polym. J*., **2002**, *38*, 947.
154. S. Bhadra and D. Khastgir. *Polymer Testing*, **2008**, *27*, 851.
155. E.A. Sanches, J. C. Soares, A. C. Mafud, G. Trovati, E. G. Fernandes, and Y. P. Mascarenhas. *J. Mol. Struct*., **2013**, *1039*, 167.
156. E. A. Sanches, L. C. A. Gomes, J. C. Soares, G. R. da Silva, and Y. P. Mascarenhas. *J. Mol. Struct*., **2014**, *1063*, 336.
157. Y. Zhou, J. Geng, G. Li, E. Zhou, L. Chen, and W. Zhang. *J. Polym. Sci.: Part B*, **2006**, *44*, 764.
158. G. R. Mitchell. *Polym. Commun*., **1986**, *27*, 346.
159. G. R. Mitchell and A. Geri. *J. Phys. D: Appl. Phys*., **1987**, *20*. 1346.
160. G. R. Mitchell, F. J. Davis and M. S. Kiani. *Br. Polym. J*., **1990**, *23*, 157.
161. S. Pruneanu, W. Graupner, L. Oniciu, M. Brie, and R. Turcu. *Mater. Chem. Phys*., **1996**, *46*, 55.
162. S. Pruneanu, R. Resel, G. Leising, M. Brie, W. Graupner, and L. Oniciu. *Mater. Chem. Phys*., **1997**, *48*, 240.
163. M. Yamaura, T. Hagiwara, and K. Iwata. *Synth. Met*., **1988**, *26*, 209.
164. K. S. Jang, B. Moon, E. J. Oh, and H. J. Hong. *Polymer-Korea*, **2003**, *27*, 323.
165. C. O. Yoon, H. K. Sung, J. H. Kim, E. Barsoukov, J. H. Kim, H. Lee. *Synth. Met.*,**1999**, *99*, 201.
166. M. R. Warren and J. D. Madden. *Synth. Met*., **2006**, *156*, 724
167. R. G. Davidson, L. C. Hammond, T. G. Turner, and A. R. Wilson. *Synth. Met*., **1996**, *81*, 1.
168. A. Ashrafi, M. A. Golozar, M.A. S. Mallakpour. *Synth. Met*., **2006**, *156*, 1280.